

# COMPARISON OF THE OPTIMAL RISK-BASED DESIGN OF PLANAR RC FRAMES WITH DIFFERENT ASPECT-RATIOS UNDER PROGRESSIVE COLLAPSE

LUCAS D.R. RIBEIRO<sup>\*</sup>, ANDRÉ T. BECK<sup>†1</sup>, FULVIO PARISI<sup>†2</sup> AND HENRIQUE M. KROETZ<sup>†3</sup>

<sup>\*</sup> Dept. of Structural Engineering, University of São Paulo, Av Trabalhador São-carlense, 400, 13566-590, São Carlos, SP, Brazil, lucasribeiro@usp.br

<sup>†1</sup> Dept. of Structural Engineering, University of São Paulo, Av Trabalhador São-carlense, 400, 13566-590, São Carlos, SP, Brazil, atbeck@sc.usp.br

<sup>†2</sup> Dept. of Structures for Engineering and Architecture, University of Naples Federico II, Via Claudio, 21, 80125, Naples, Italy, fulvio.parisi@unina.it

<sup>†3</sup> Center for Marine Studies, Federal University of Paraná, Av Beira Mar, s/n, 83255-976 Pontal do Parana, PR, Brazil, henrique.kroetz@ufpr.br

**Key words:** kriging, progressive collapse, reinforced concrete, risk optimization, uncertainty.

**Summary.** A sudden failure of a single supporting element within a reinforced concrete (RC) frame can lead to a disproportionate collapse if the design lacks mechanisms to confine initial damage through resisting mechanisms. Given the substantial impact of uncertainties related to material properties and geometric parameters on these mechanisms, coupled with the high stakes associated with such failures, the risk-based optimization offers a practical approach to achieving a balance between cost-efficiency and safety. Besides, optimal risk-based design is strongly dependent on the structural configuration. This study exemplifies this approach by optimizing five RC frames under three scenarios of column removal on the first floor: middle column, penultimate column, and corner column. Design variables encompass cross-sectional depth, steel rebar areas, and concrete strength of beams and columns. Failure consequences are evaluated for both the intact structure and all column removal scenarios. Conducting a physical and geometrical nonlinear static analysis, sample points undergo bay pushdown analysis in OpenSees software. Addressing failure probabilities utilizes the Weighted Average Simulation Method, with risk optimization performed by the Firefly Algorithm. To mitigate computational costs arising from nonlinearities and a high number of required sample points, surrogates are used to quickly estimate limit states and reliability indexes. Results contrasts with the observed trend in Beck et al. [1], with optimal beam strengthening not varying in terms of the frame's aspect ratio.

## 1 INTRODUCTION

Progressive collapse happens when an initial member failure triggers the failure of the adjacent elements, in resemblance to a cascade effect, leading to a final failure with a disproportionate higher severity in relation to the initial event [2]. When under multiple hazards, the probability of structural collapse  $P[C]$  is given as:

$$P[C] = \sum_H \sum_{LD} P[C|LD, H] P[LD|H] P[H] \quad (1)$$

where  $P[H]$  is the probability of hazard occurrence;  $P[LD|H]$  is the conditional probability of local damage for a given hazard  $H$ ; and  $P[C|LD, H]$  is the conditional probability of collapse for a given  $LD$  and  $H$ .

This study follows Beck et al. [1, 3], considering  $P[LD|H] P[H]$  as the probability of local damage  $P_{LD}$  to combine column loss and intact structure scenarios in a single objective function related to total expected costs  $C_{TE}$ . Hence, the cost-benefit of considering column removal scenarios in designing RC frames while considering the realistic nonlinear structural behavior is then addressed.

Based on Beck et al. [1], this work focuses on investigating the influence of the frame aspect ratio over the optimal risk-based design. More specifically, it is investigated if the preference for optimal stronger beams in taller frames and weaker beams in lower frames is also shown when addressing a nonlinear capacity model for progressive collapse simulation.

Five RC frames with distinct aspect ratios (number of bays x number of stories) are the objects of study. All frames have similar “tributary” area in terms of number of bays multiplied by the number of stories (Figure 1). Each frame has beam spans of 6.00 m and column interstory height of 3.00 m, and each frame is subjected to 4 scenarios: intact structure, loss of exterior column at ground floor, loss of penultimate column at ground floor, and loss of middle column at ground floor. Each column loss scenario is treated individually, so local damage probability  $P_{LD}$  relates to the sudden loss of one column at a time.

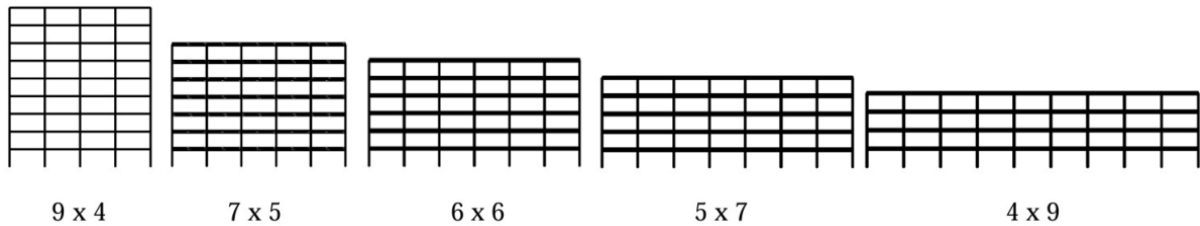


Figure 1: Objects of study

## 2 PROPOSED FRAMEWORK

Based on Beck et al. [1,3], a threat-independent approach is adopted, combining hazard probability and column loss probability conditional to hazard as probability of local damage  $P_{LD} = \sum_H P[CL|H]P[H]$ . To comprehend how progressive collapse influences the optimal risk-based design for each frame,  $P_{LD}$  is assumed to range between a lower value  $P_{LD}^{min} = 5 \times 10^{-6}$  to 1. This allows to cover scenarios gradually changing from negligible to significant threat of column loss. It is noteworthy to mention that  $P_{LD}^{min}$  relates to the 50-year lifespan equivalent to the “de minimis” annual probability  $p = 10^{-7}$  [4].

The adopted framework relies on four pillars (Figure 2):

- (a) risk-based optimization: total expected costs, given by cost of construction and expected costs of failure, are minimized for each  $P_{LD}$  via Firefly Algorithm [5];
- (b) reliability analysis: in order to compute the expected costs of failure, probability of occurrence for each failure mode is addressed by Weighted Average Simulation Method (WASM) [6];
- (c) structural modeling: at each sample point, structural response is addressed via nonlinear FEM for limit state evaluation with OpenSees [7];
- (d) surrogate usage: as structural and reliability analyses have great computational burden, simplified yet accurate estimations via Inverse Distance Weighting (IDW) [8] are used to hasten these stages.

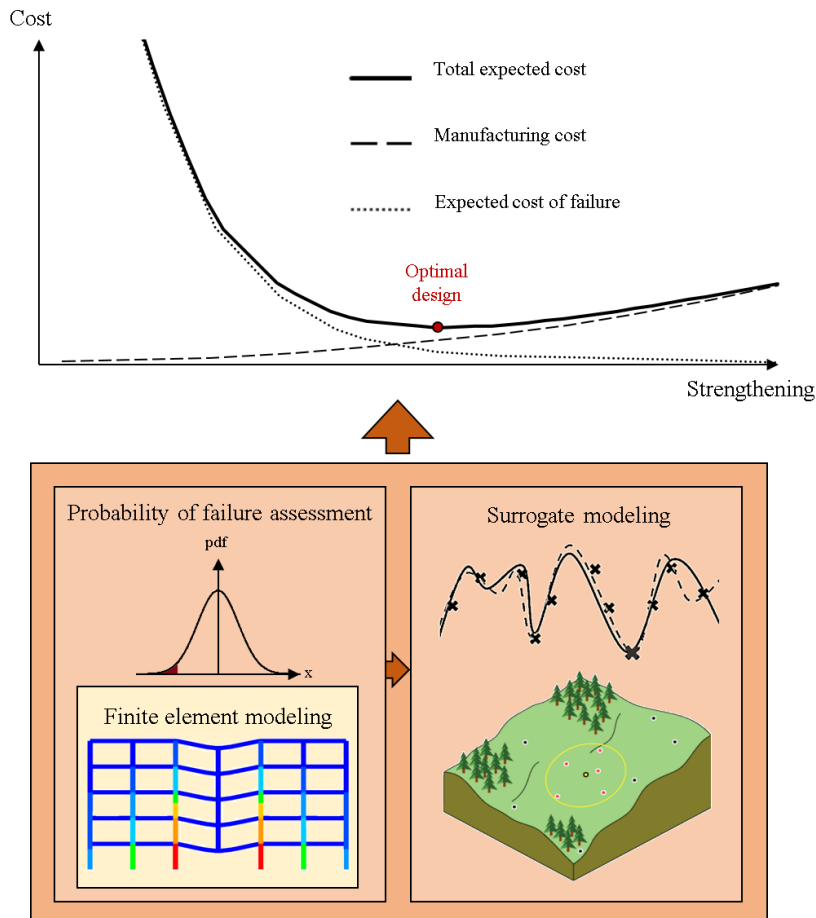


Figure 2: Proposed framework

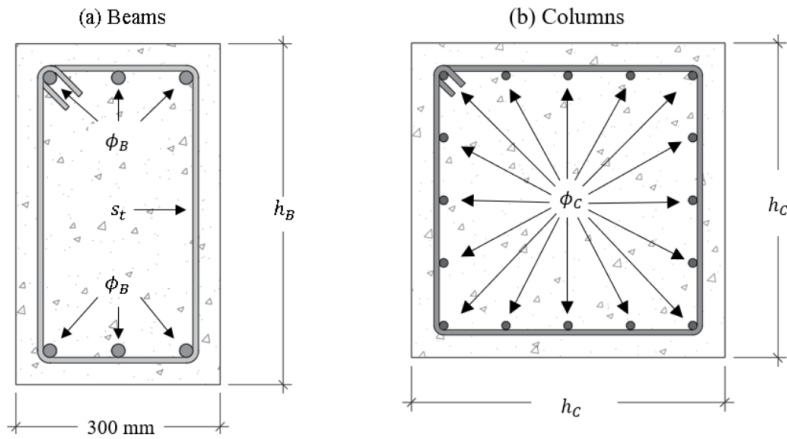
The primary frames of Figure 1 are extracted from the interior of the building, so unidirectional floor slabs lead to floor loadings from both sides. Although facade columns at ground floor are more exposed for certain hazards, such as IEDs and vehicular impacts, it is herein assumed buildings with easy access at ground floor. Hence, admitting terrorist attacks as potential hazard, inner column spans are also prone to malicious intentions.

The total expected cost  $C_{TE}$  (Eq. 2) to be minimized (via Eq. 3) addresses manufactural costs and the expected costs of all failure modes. Additional life-cycle costs could be included in  $C_{TE}$ , but they are out of the scope of this manuscript.

$$C_{TE}(\mathbf{X}, \mathbf{d}) = C_M + \sum_{i=1}^{NIF} k_i P_{fi} C_{MAi} + \sum_{k=1}^{NCL} \sum_{j=1}^{NCLF} k_j P_{fj} C_{MAj} P_{LDk} \quad (2)$$

$$\begin{aligned} & \text{find } \mathbf{d}^* \\ & \text{which minimizes } C_{TE}(\mathbf{X}, \mathbf{d}) \\ & \text{subject to } \mathbf{d} \in \mathcal{D} \end{aligned} \quad (3)$$

In Eq. 2,  $C_M$  is the construction cost;  $NIF$  and  $NCLF$  represent the number of failure modes for intact and each column loss scenario, respectively; and  $NCL$  stands for the number of column loss scenarios. Vector  $\mathbf{X}$  relates to the random variables, while vector  $\mathbf{d}$  corresponds to the mean value to be optimized for each random design variable. Parameter  $C_{MA}$  refers to the construction cost of the areas damaged by a given failure mode. Multipliers  $k$  relate to the severity of each failure mode (Table 2). As shown in Figure 3, design variables  $\mathbf{d}$  are the beam depth  $h_B$ , beam rebar diameter  $\phi_B$  (symmetric bottom and top rebars), beam stirrup spacing  $s_t$ , column size  $h_C$  (square column), column rebar diameter  $\phi_C$ , and overall concrete strength  $f'_C$ .



**Figure 3:** Design variables.

Rebars are assumed symmetric to facilitate results comprehension given the greater complexity of addressing and comparing multiple frames. Besides, a seemingly exaggerated number of 16 columns rebars is chosen to ensure that a unique detailing is able to cover all frames in all scenarios given the design domain  $\mathcal{D}$ , which is favorable in terms of direct comparisons between distinct frames.

Reinforcing the entire frame is the only progressive collapse mitigating strategy addressed, as the scope of this example relies in exclusively addressing aspect ratio influence. Based on Starossek and Haberland [9], structural segmentation could be more appropriate for the horizontally aligned frames than an APM design, but this is avoided to allow an initial direct comparison between frames.

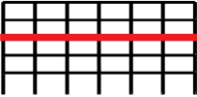

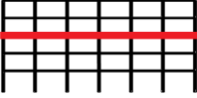
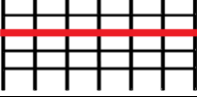
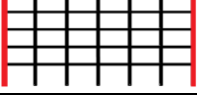
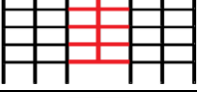
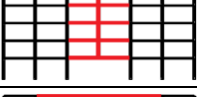

The probability of occurrence of each failure mode for each column loss scenario and frame configuration is estimated via IDW [8], which relies on 2000 design support points with failure probabilities computed via WASM [6]. Table 1 shows the uncertainty modelling for reliability analysis at the design support points. A sample with 30 million points is enough to ensure probability convergence for each failure mode, 2000 design support points, and for each frame.

Each sample point created via LHS has its limit states computed as shown in Table 2, with the most relevant internal forces and ultimate load capacity at CA estimated via IDW. The parameters obtained via IDW refer to the static pushdown curve, so Energy Equivalence Method [10] is used to obtain these parameters in terms of the Pseudo-static pushdown curve in order to address the dynamic effects. This initial metamodeling stage relies on 2000 limit state support points, which are analyzed in OpenSees.

**Table 2:** Uncertainty modeling

Category	RV	Distribution	Mean	Standard deviation	Coefficient of variation
Geometry	Beam depth ( $h_B$ )	Normal	To be optimized*	1 mm	-
	Beam rebar diameter ( $\phi_B$ )	Normal	To be optimized*	-	0.05
	Stirrup spacing ( $s_t$ )	Normal	To be optimized*	-	0.05 (assumed)
	Column size ( $h_C$ )	Normal	To be optimized*	1 mm	-
	Column rebar diameter ( $\phi_C$ )	Normal	To be optimized*	-	0.05
Material	Concrete strength ( $f'_c$ )	Lognormal	To be optimized*	-	0.12
	Rebar yield strength ( $f_y$ )	Normal	510 MPa	-	0.05
	Concrete unit weight ( $\gamma_c$ )	Normal	25 kN/m <sup>3</sup>	-	0.05 (assumed)
	Ultimate steel strain ( $\epsilon_{su}$ )	Normal	0.20	-	0.14
Loads	Dead load ( $D$ )	Normal	$1.05D_n$	-	0.10
	50-year live load ( $L_{50}$ )	Gumbel	$1.00L_n$	-	0.25
	Arbitrary point in time live load ( $L_{apt}$ )	Gamma	$0.25L_n$	-	0.55
Structural model	Model error ( $M_E$ )	Lognormal	1.101	0.187	-

**Table 2:** Failure modes.

Case	Failure mode	$k$	Limit state function	Damaged area
Intact structure ( $I$ )	Large deflection	5	$g_{I,SE}(\mathbf{x}) = \delta_{lim} - \delta(q_I)$	
	Bending failure at midspan	30	$g_{I,BM}(\mathbf{x}) = M_{RM} - M_M(q_I)$	
	Bending failure at beam ends	30	$g_{I,BE}(\mathbf{x}) = M_{RE} - M_E(q_I)$	
	Shear failure	60	$g_{I,SH}(\mathbf{x}) = V_R - V(q_I)$	
	Column failure	60	$g_{I,COL}(\mathbf{x}) = R(N_R, M_R) - S(N_{SI}, M_{SI})$	
Column loss ( $CL_i$ )	Rebar rupture	40	$g_{CL_i,SR}(\mathbf{x}) = q_{CL_i,SR} - \tilde{q}_{CL}$	
	Shear failure	60	$g_{CL_i,SH}(\mathbf{x}) = V_R - V(\tilde{q}_{CL})$	
	Column failure	80	$g_{CL_i,COL}(\mathbf{x}) = R(N_R, M_R) - S(\tilde{N}_{SCLi}, \tilde{M}_{SCLi})$	

Each beam span is discretized in 5 fiber displacement-based finite elements (3 Lobatto integration points in each), being 3 finite elements for the member itself and 1 at each end to represent the joint region. Praxedes [11] shows the efficiency of this approach in terms of minimal refinement level and agreement with experimental static pushdown curves.

Corrotational transformation is used for all beam and column elements to account for the expected large geometrical nonlinearities. Cross-section layering consists of 200 fibers for the confined concrete and 10 fibers for each face of unconfined concrete cover. Static bay pushdown analysis is performed with a displacement-based integrator using Kylov-Newton method to solve the nonlinear problem (tolerance of  $10^{-5}$ ). An initial increment size of 1 mm is adopted, but an adaptive algorithm is used to enhance or decrease the step depending on the lack or need of convergence improvement, respectively.

Since in bay pushdown analysis [12] only the beam spans adjacent to the lost column have an increasing load applied, two load steps are adopted: a) nominal dead and live load are applied over all beam spans, as well as the self-weight of each structural member on itself; b) if beam rebar rupture does not occur on the first stage (possible for weak beam configurations), an increasing load is applied over the beam spans of interest until rebar rupture is verified.

The modified Park-Kent model [13] is used as reference to estimate the confined and unconfined concrete behavior in compression, and the multilinear model from fib Model Code [14] is the reference for concrete in tension. All main parameters from both models are used as inputs for the “concretewBeta” model available in OpenSees, relying on cross-section geometry,  $f'_c$  and stirrup detailing to be inferred.

Rebar behavior is represented by the “ReinforcingSteel” model, which realistically encompasses the linear elastic region, the yield plateau, strain hardening, and strain softening which are expected for typical steel reinforcements. Usual bilinear models are not used due a fixed value of hardening modulus of elasticity  $E_{sh}$  being adopted, which leads to load x displacement discrepancies and unrealistic rebar stresses for advanced stages of catenary action.

### 3 RESULTS

Figure 4 shows the increase in beam capacity in terms of the optimal risk-based results for each frame configuration under each individual columns loss scenario. In Figure 4, external, penultimate and middle column loss scenarios are represented by  $ECL$ ,  $PCL$  and  $MCL$ , respectively;  $BM$  relates to bending capacity and  $SH$  to shear capacity. Since rebars are symmetric, no distinction is made between positive or negative bending capacity.

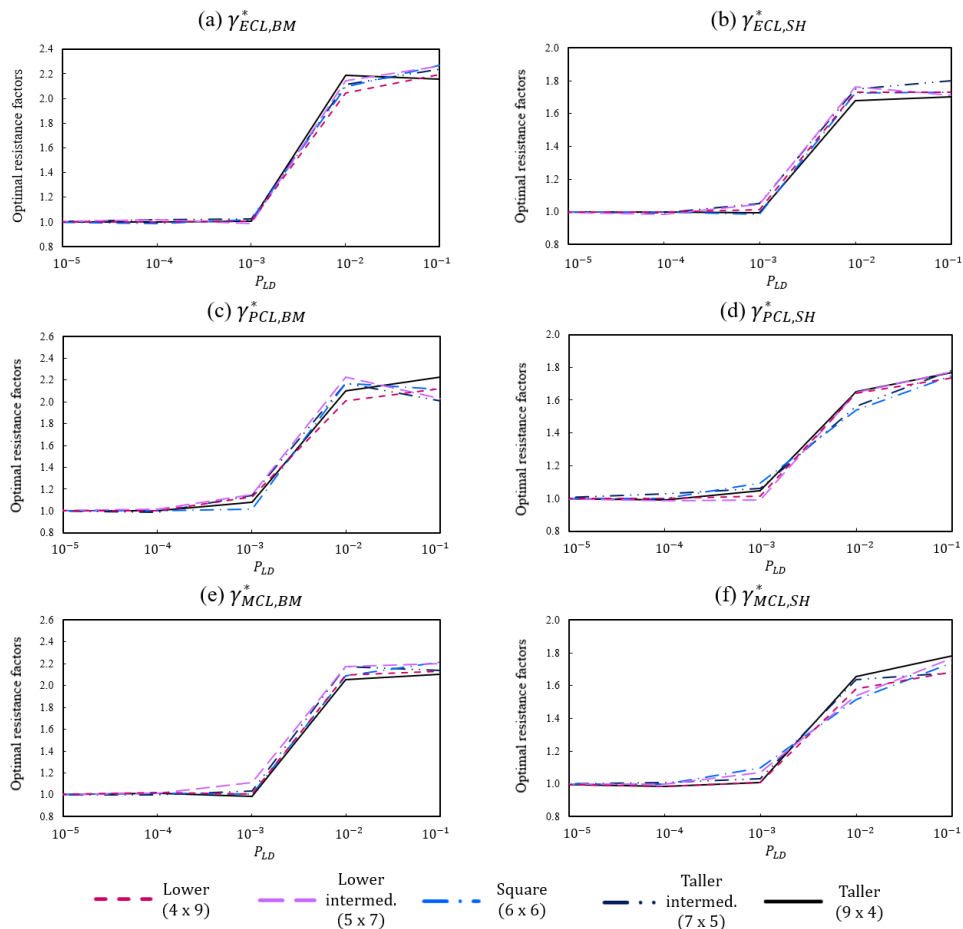


Figure 4: Optimal beam resistance factors.

Optimal risk-based designs related to a Normal Loading Condition are constant from  $P_{LD}^{min}$  up to  $P_{LD} \approx 10^{-3}$  (1st stage), after which a threshold  $P_{LD}^{th}$  is identified in all cases. Past this point, APM design against progressive collapse becomes cost-effective, defining a 2nd stage.

Optimal 1st stage beam design is: beam depth up to its upper bound, rebar ratio of 0.42%, and stirrup ratio of 0.17%. Load combination  $q_I = 1.2D_n + 1.6L_n$  leads to roughly 64 kN/m over the beam spans. Hence, DCRs are obtained as follows: 1.03 for bending at the beam ends ( $\phi = 0.9$ ); 0.52 for bending at the midspan ( $\phi = 0.9$ ); and 0.82 for shear failure ( $\phi = 0.75$ ). As symmetric rebars are adopted, more than enough safety is shown against midspan bending.

Optimal 1st stage column design shows an expected increased capacity for taller frames. Combination for usual loading condition  $q_I = 1.2D_n + 1.6L_n$  leads to roughly 64 kN/m in the beam spans (6 m) and 4.8 kN/m for column spans (3 m). At floor level, it is roughly expected 1550 kN for the lowest frame (4 x 9); 2000 kN for the lower intermediate frame (5 x 7); 2330 kN for the squared frame (6 x 6); 2800 kN for the taller intermediate frame (7 x 5); and 3600 kN for the tallest frame (9 x 4). These expected axial demands correspond to 0.36, 0.48, 0.56, 0.52 and 0.59 of the respective optimal axial column capacities, and a minimum eccentricity of 20 mm still keeps each axial load x moment demand inside the column resisting envelope. The top corner of each frame presents negligible axial forces and bending moments of  $\sim 0.05$  of its greatest axial demand. By comparing these demands with the columns optimal resisting envelopes, DCRs ranging from 1.2 (taller frame) to 0.77 (lower frame) are obtained.

Hence, lower safety margins are allowed for column failure as the frame height increases, reaching  $DCR > 1$  at the frame top corner ( $\phi = 0.9$ , as demand is mainly flexural) and  $\sim 0.91$  at the ground floor ( $\phi = 0.65$ ) for the tallest frame configuration. As the column cost/meter increases for taller frames, cost-effectiveness of avoiding column plastification reduces for the intact structure, especially at the top corner of the frames.

Overall concrete strength  $f'_c$  shows the same multipurpose characteristics of the beam depth  $h_B$ . Although it does not influence the pushdown behavior, an increased  $f'_c$  directly provides greater resistance against 5 failure modes: serviceability, negative and positive beam bending, shear failure and column failure. Therefore, ensuring  $f'_c^*$  at its upper bound in  $\mathcal{D}$  (45 MPa) for all frames in all scenarios is shown to be the choice of best cost-effectiveness.

Optimal 2nd stage beam design is similar for all frames and all column loss scenarios, with beam depth equal to its upper bound, maximum concrete strength, rebar ratios up to 1.03%, and stirrup ratio up to 0.50%. By addressing a Dynamic Amplification Factor (DAF) of 1.22 (common value between CAA and CA in pseudo-static pushdown curves), load combination for extraordinary loading condition  $q_{CL} = 1.25(1.2D_n + 0.5L_n)$  leads to roughly 64 kN/m over the beam spans ( $D_n = 3\text{kN/m}^2$  and  $L_n = 2\text{kN/m}^2$ ). Overall DCR factors related to ultimate beam capacity are  $\sim 0.9$ , indicating a rebar rupture safety margin of  $\sim 10\%$  for all frames for all column loss scenarios. Since DCR relates to a material property, no strength reduction factor  $\phi$  is used.

Overall increase in optimal bending capacity is around 2.2 for  $P_{LD} > P_{LD}^{th}$ , whilst for shear capacity it is 1.8. Although lower frames have a smaller damaged area in case of upward collapse propagation due to beam failure, weaker beams are never shown to be justified, in contrast with Beck et al. [1]. In the mentioned study, a progressive collapse capacity model that neglects the bending moments over adjacent columns shows that stronger beams are only cost-effective for taller frames, where the upward collapse propagation is as severe as horizontal column collapse propagation.



However, realistic capacity models reveal that significant axial forces developed during Catenary and Vierendeel Actions have major impacts over adjacent columns. Besides weak beams having lower ultimate capacity, Vierendeel and Catenary Action develop earlier, leading to larger bending moment demands over the adjacent columns.

These additional flexural demands increase the propensity of column rebar yielding. In case of tensile column rebar yielding, full achievement of beam ultimate capacity is severely compromised, while compressive column rebar yielding also leads to a brittle and sudden column collapse. This justifies the risk-based algorithm's preference for stronger beams independently of the frame configuration or column loss scenario.

#### 4 CONCLUSIONS

- Cost-effectiveness of progressive collapse mitigation strategies is found to strongly depend on threat probabilities for all frames and column loss scenarios.
- A transition in optimal solutions was observed, with optimal cross-sections changing from a configuration with best performance under normal loading condition to another with best performance against progressive collapse, characterizing the threshold local damage probability  $P_{LD}^{th}$ .
- When the abnormal load and threat are such that  $P_{LD} < P_{LD}^{th}$ , APM design for load bridging is not cost-effective. By contrast, APM design pays off under significant threat probabilities, with strengthening costs being compensated by a reduction in expected costs of failure.
- Under prevalence of usual loading condition, the risk-based framework leads to a good balance between safety and construction cost, allocating material to provide just-enough safety against the most critical failure modes, namely bending at the beam ends and column failure.
- Increased ultimate capacity is ensured for  $P_{LD} > P_{LD}^{th}$ , with rebar and stirrup reinforcements of larger ratios, and concrete strength up to its upper bound.
- Weaker columns result in optimal APM beam designs with greater depth.
- As it is not cost-effective to ensure greater column capacity in 2nd stage, ultimate frame capacity solely relies on increasing the beam depth in order to avoid magnified bending moments over the vertical elements.
- Beck et al. [1] show optimal APM designs characterized by weaker beams for lower frames and stronger beams for taller frames. Yet, this is solely related to the estimated consequences from an upward progression of collapse due to beam failures. When addressing the entire system behavior, weaker beams are never shown to be justified.

#### ACKNOWLEDGEMENTS

Funding of this research project by FAPESP (grant n. 2019/23531-8 and grant n. 2021/12884-7) and joint FAPESP-ANID (São Paulo State Foundation for Research - Chilean National Agency for Research and Development, grant n. 2019/13080-9).

## REFERENCES

- [1] A. T. Beck, L. d. R. Ribeiro, M. Valdebenito and H. Jensen. Risk-based design of regular plane frames subject to damage by abnormal events: A conceptual study. *Journal of Structural Engineering*, 148(1): 04021229, 2022.
- [2] F. Parisi; N. Augenti. Influence of seismic design criteria on blast resistance of RC framed buildings: A case study. *Engineering Structures*, Elsevier, 44: 78-93, 2012.
- [3] A. T. Beck, L. d. R. Ribeiro and M. Valdebenito, M. Risk-based cost-benefit analysis of frame structures considering progressive collapse under column removal scenarios. *Engineering Structures*, Elsevier, 225: 111295, 2020.
- [4] E. Pate-Cornell. Quantitative safety goals for risk management of industrial facilities. *Structural Safety*, Elsevier, 13(3): 145–157, 1987.
- [5] X. S. Yang. *Nature-Inspired Metaheuristic Algorithms*. UK: Luniver Press, 2008.
- [6] M. Rashki, M. Miri, M. Moghaddam. A. A new efficient simulation method to approximate the probability of failure and most probable point. *Structural Safety*, Elsevier, 39: 22-29, 2012.
- [7] F. T. Mckenna, M. H. Scott and G. L. Fenves. Nonlinear finite-element analysis software architecture using object composition. *Journal of Computing in Civil Engineering*, ASCE, 24(1): 95-107, 2010.
- [8] D. Shepard. A two-dimensional interpolation function for irregularly-spaced data. In: *Proceedings of the 1968 23rd ACM national conference*: 517-524, 1968.
- [9] U, Starossek and M. Haberland. Disproportionate collapse: Terminology and procedures. *Journal of Performance of Constructed Facilities*, ASCE, 24(6): 519–528, 2010.
- [10] G. Q. Xu and B. R. Ellingwood. An energy-based partial pushdown analysis procedure for assessment of disproportionate collapse potential. *Journal of Constructional Steel Research*, Elsevier, 67(3): 547-555, 2011.
- [11] C. S. N. Praxedes. Robustness-based optimal progressive collapse design of RC frame structures. Thesis (PhD – Civil Engineering) – Ryerson University, Toronto, Ontario, Canada, 2020.
- [12] K, Khandelwal and S. El-Tawil. Pushdown resistance as a measure of robustness in progressive collapse analysis. *Engineering Structures*, Elsevier, 33: 2653-2661, 2011.
- [13] R. Park, M. J. N. Priestley and W. D. Gill. Ductility of square-confined concrete columns. *Journal of Structural Engineering*, ASCE, 108(ST4): 929-950, 1982.
- [14] Comité Euro-International du Béton. CEB-FIP. Model Code 2010: Final Draft. *Bulletin D'information*, CEB, Lausanne, 2011.